Synthesis of chitosan zero-valent iron nanoparticles-supported for cadmium removal: characterization, optimization and modeling approach

Mehdi Ahmadi, Majid Foladivanda, Nemat Jaafarzadeh, Zahra Ramezani, Bahman Ramavandi, Sahand Jorfi and Babak Kakavandi

ABSTRACT

Herein, chitosan (CS) impregnated with nanoparticles of zero-valent iron (NZVI) was fabricated onto a magnetic composite of CS@NZVI as an adsorbent for cadmium (Cd^{2+}) removal from aqueous solution. The characteristics of CS@NZVI were analyzed by Fourier transform infrared spectroscopy, X-ray diffraction, transmission electron microscopy, CHONS and Brunauer, Emmett and Teller techniques. The average diameter of NZVI was found to be 50 nm, and it was successfully coated onto the CS. The influential experimental variables such as contact time, solution pH, adsorbent dosage and initial Cd^{2+} concentration were investigated to determine optimum conditions. Results revealed that with an optimum dosage rate of 0.6 g/L, Cd^{2+} concentration was reduced from 10 to 0.016 mg/L within 90 min reaction time at pH of 7 ± 0.2. Experimental data were fitted to the Freundlich and pseudo-second-order models. Maximum adsorption capacity was obtained from the Langmuir monolayer 142.8 mg/g. Desorption experiments showed that the CS@NZVI had good potential with regard to regeneration and reusability, and its adsorption activity was preserved effectively even after three successive cycles owing to its good stability. As a conclusion, CS@NZVI can be considered as an effective adsorbent for heavy metals removal from water and wastewaters, because it can be separated both quickly and easily, it has high efficiency, and it does not lead to secondary pollution.

Key words | adsorption, cadmium, chitosan, magnetic composite, ZVI nanoparticles

Mehdi Ahmadi
Nemat Jaafarzadeh
Sahand Jorfi
Babak Kakavandi (corresponding author)
Environmental Technologies Research Center,
Ahvaz Jundishapur University of Medical Sciences,
Ahvaz,
Iran
E-mail: *Kakavandi.b@ajums.ac.ir*

Zahra Ramezani
Nanotechnology Research Center,
Ahvaz Jundishapur University of Medical Sciences,
Ahvaz,
Iran

Mehdi Ahmadi
Majid Foladivanda
Nemat Jaafarzadeh
Sahand Jorfi
Babak Kakavandi
Department of Environmental Health Engineering,
Ahvaz Jundishapur University of Medical Sciences,
Ahvaz,
Iran

Bahman Ramavandi
Department of Environmental Health Engineering,
Bushehr University of Medical Sciences,
Ahvaz,
Iran

Babak Kakavandi
Student Research Committee,
Ahvaz Jundishapur University of Medical Sciences,
Ahvaz,
Iran

INTRODUCTION

Heavy metals are highly toxic and hazardous elements that have a high atomic weight and a density at least 5 times greater than that of water. They are widely used in industrial, domestic, agricultural, medical and technological applications, which has led to their continuous release into the environment. Due to their high degree of toxicity, arsenic (As), cadmium (Cd), chromium (Cr), lead (Pb) and mercury (Hg) rank among the priority metals that are of public health significance (Jaafarzadeh *et al.* 2012; Begum *et al.* 2016). Cadmium (Cd^{2+}) is one of the most dangerous pollutants that is released into the environment, mainly via industrial applications such as phosphate fertilizers, batteries, electroplating industries, mining, metal production, stabilizers and alloys and the manufacturing of pigments. It has been classified as a human carcinogen and teratogen impacting lungs, kidneys, liver and reproductive organs (Azari *et al.* 2015; Naghizadeh 2015). The World Health Organization (WHO) has set a maximum guideline concentration of 0.003 mg/L for Cd^{2+} in drinking water (WHO 2007). Considering the negative effects, toxicity and stability of heavy metals, their complete removal from water resources and wastewater effluents is deemed necessary.

doi: 10.2166/aqua.2017.027

In the last several years, different technologies have been studied to remove heavy metals from aqueous solutions including adsorption, ion exchange, chemical precipitation, membrane filtration and coagulation–flocculation (Azari *et al.* 2015). However, most of them suffer from several disadvantages such as higher operational and capital costs, more energy and chemicals consumption, and problems regarding sludge disposal (Sobhanardakani *et al.* 2015). Other drawbacks are the requirement for large settling tanks in chemical precipitation, regeneration in the ion exchange process, chemical requirements, low efficiency in coagulation–flocculation methods and large amounts of sludge in membrane filtration (Gupta *et al.* 2011b; Kakavandi *et al.* 2015). During the past few years, the adsorption process has been widely applied; also, this process is proven to be a suitable method for the treatment of heavy metals (Ahmadi *et al.* 2011; Amiri *et al.* 2011). In this regard, up to now, a wide variety of adsorbents have been used for Cd^{2+} removal such as agricultural waste biomass, chitosan–silica, microorganisms, biopolymers, zeolites, metal oxides, fly ash and activated carbon (Jaafarzadeh *et al.* 2014; Lim & Aris 2014).

However, most of these adsorbents showed a relatively low adsorption capacity for Cd^{2+} under the optimum operation conditions. In addition, some operational problems such as resultant turbidity in the treated water or effluent, and consequently the need to filter or centrifuge, have limited the application of these adsorbents, particularly nano-sized adsorbents. Magnetic nanoparticles (e.g. NZVI, Fe_3O_4, α-Fe_2O_3, γ-Fe_2O_3 and FeO(OH)) have recently been adopted by researchers in the field of adsorption/biosorption for removing pollutants from aquatic environments, which makes separation of both adsorbent and adsorbate much easier (Mohseni-Bandpi *et al.* 2015). Several authors have magnetized adsorbents such as activated carbon for Pb^{2+} and Hg adsorption (Oliveira *et al.* 2002; Kakavandi *et al.* 2015), carbon nanotubes for Pb^{2+}, Ni and Sr adsorption (Chen *et al.* 2009; Hu *et al.* 2010), zeolite for Cr, Cu, and Zn adsorption (Oliveira *et al.* 2004) and CS for Zn^{2+} and Pb^{2+} adsorption (Fan *et al.* 2011, 2013) by magnetic iron nanoparticles as a magnetic separation technology.

Among magnetic nanoparticles, NZVI has been applied recently for in-situ and ex-situ remediation, due to being non-toxic and inexpensive (Esfahani *et al.* 2014a). NZVI, due to its extremely small particle size, large specific surface area and greater reactive sites and capacity, is notable for this purpose in wastewater treatment to remove heavy metals with a higher efficiency (Esfahani *et al.* 2014b). Moreover, the magnetic properties of NZVI facilitate the rapid separation of nano iron from soil and water via a magnetic field (Babaei *et al.* 2015a). However, there is a strong tendency of NZVI particles to agglomerate as well as to become oxidized, resulting in a reduction in surface area, reactivity and removal efficiency (Babaei *et al.* 2015a). An effective approach to overcome this problem is to incorporate NZVI into a porous supporting material. Recent studies have reported that NZVI particles can be coated with CS (a protective polymer due to its outstanding chelation behavior) to increase its dispersibility and stability (Liu *et al.* 2012). Furthermore, these supports can facilitate the separation of NZVI particles from aqueous solutions.

Herein, we hypothesize that NZVI particle impregnation on the CS surface combines the synergistic effects of NZVI and CS, which may have a superbly enhanced adsorption activity as well as easy separation. The present study therefore aimed to synthesize CS@NZVI using a liquid phase method. The influence of operating parameters in the adsorptive removal of Cd^{2+} was evaluated in details in a batch system. Isothermic and kinetic studies were also carried out under optimum conditions. Finally, the regeneration and reusability of the composite were indeed evaluated for three consecutive cycles.

MATERIALS AND METHODS

Materials and chemicals

All chemicals were of analytical laboratory grade and used without further purification. Sodium borohydride ($NaBH_4$) was purchased from Sigma-Aldrich. Cadmium nitrate tetrahydrate ($Cd(NO_3)_2.4H_2O$, Merck, Co) was used for preparing the stock solutions of Cd^{2+} according to the ASTM D3557-12 (ASTM 2012) procedure. The pH of the solutions was adjusted by adding 0.1 M hydrochloric acid (HCl) and sodium hydroxide (NaOH) solutions. All the

reagents were prepared with de-ionized water (DI-water) and kept in a refrigerator at 4 °C prior to experiments.

CS preparation

In this work, CS was prepared from shrimp shell wastes, which is available in abundance in southern parts of Iran. It was obtained from chitin according to the method reported in the literature with some modifications (Brown 2015). Initially, in order to improve the purity of shrimp shells, they were washed with DI-water and dried, then ground and passed through a size 50 mesh. Graded shells were agitated in 0.5% NaOH solution for 30 min and finally washed with hot DI-water several times until pH reached neutral value. This completed the preliminary phase for the preparation of chitin. De-proteinization of the shrimp shells was performed using a 1.2N NaOH solution (1:20 w/v) for 3 h at 90 °C and in constant agitation conditions. The residue was separated by filtration and washed with hot DI-water several times. Thereafter, it was demineralized with a 1.6N HCl solution (1:10 w/v) at room temperature (25 ± 2 °C) for 2 h. After filtration, the residue was again washed with hot DI-water until the pH reached 7. Finally, the obtained chitin was decolorized via agitation in acetone solution [$(CH_3)_2CO$] for 1 h in order to remove all pigments. Chitin was separated, dried at 60 °C for 24 h and then weighed to determine the chitin content of the shrimp shells according to Equation (1) (Westergren 2006). Afterwards, the obtained chitin was de-acetylated using a 50% NaOH (1:5 w/v) solution at boiling temperature for 8 h. After de-acetylation, the produced CS was washed with DI-water until the pH reached 7, and dried in an oven at 60 °C for 24 h. Thereafter, it was weighed and the CS yield was determined using Equation (2), and assayed for degree of de-acetylation. One of the easiest ways to detect CS production is dissolving in a weak acid solution as an indicator test (Westergren 2006; Brown 2015).

$$\%\text{Chitin} = \frac{\text{Product (g)}}{\text{Shell (g)}} \times 100 \quad (1)$$

$$\%\text{Chitosan} = \frac{\text{Product (g)}}{\text{Shell (g)}} \times 100 \quad (2)$$

Synthesis of the CS@NZVI

CS@NZVI composite was synthesized in the laboratory using a chemical reduction method (reducing Fe^{3+} to Fe^0 using $NaBH_4$). Excess $NaBH_4$ was used to ensure that all the Fe^{3+} was reduced. Firstly, 0.25 g of CS was dissolved in 50 mL of 0.05 M acetic acid. Due to the poor solubility of CS, the mixture was vortexed to aid complete dissolution and kept for 2 h at 150 rpm. To this solution, 1 g of $FeCl_3.7H_2O$ was added and the solution was stirred quickly in an N_2-purged environment for 2 h. Then, to this mixture freshly prepared aqueous solution containing 2% $NaBH_4$ was added drop-wise. At this stage, black precipitation was observed, and evolution of H_2. Again, the mixture was stirred for another 60 min until the entire reduction of metal salts. The black solid was collected using a magnet (with a 1.5 tesla filed magnet) and washed at least three times with oxygen-free DI-water to get rid of the extra chemicals. The CS@NZVI composite was dried at 100 °C for 4 h, and stored in a brown sealed bottle under dry conditions for characterization and future use (Geng *et al.* 2009; Gupta *et al.* 2011a).

Characterization of CS@NZVI

In order to determine the CS degree of acetylation, the elemental composition was analyzed using a COSTECH ECS 4010, Italia, CHONS equipment. The percentage of *N*-deacetylated varies from 5.145 in completely *N*-deacetylated CS ($C_6H_{11}O_4N$ repeat unit) to 6.861 in chitin, the fully *N*-acetylated polymer ($C_8H_{13}O_5N$ repeat unit). The DA % of CS samples was calculated via Equation (3) (Al Sagheer *et al.* 2009).

$$DA(\%) = \frac{C/N - 5.145}{6.861 - 5.145} \times 100 \quad (3)$$

X-ray diffraction (XRD) spectra of CS@NZVI were obtained using a Quantachrome, 2000, NOVA X-ray Diffractometer with graphite monochromatic copper radiation (Cu Kα, $\lambda = 1.54$ Å) in the range of 10–70°. The patterns were compared with the Joint Committee on Powder Diffraction Standards (JCPDS). The specific surface area and pore volume of CS@NZVI were measured by the Brunauer,

Emmett and Teller (BET, Quantachrome, 2000, NOVA) method using N_2 adsorption–desorption isotherms at 77.3 K. A transmission electron microscopy (TEM, PHILIPS, EM) was used to characterize the size and shape of NZVI particles at 100 keV. Fourier transform infrared spectroscopy (FTIR) spectra of the CS@NZVI composite were obtained using BRUKER's Vertex 70 model to confirm the functional groups present on the adsorbent surfaces.

Batch adsorption experiments

Batch experiments for the adsorption of Cd^{2+} on CS@NZVI composite were carried out in 250 mL polytetrafluoroethylene bottles filled with 50 mL of the pH-adjusted Cd^{2+} solutions at $25 \pm 1\ ^{\circ}C$. The effects of experimental parameters such as the pH of the solution, contact time, different CS@NZVI and Cd^{2+} concentrations and solution temperatures on the removal efficiency of Cd^{2+} were investigated. After adjusting the pH of the solution, a specific amount of composite was put in the aqueous solution, having a fixed concentration. Then, bottles were agitated on a rotary shaker at a rate of 200 rpm and maintained for a certain period of time at a constant temperature ($25 \pm 1\ ^{\circ}C$). At appropriate time intervals, 2 mL of the solution was withdrawn from each bottle and the composite was magnetically separated using a strong magnet. After that, the remaining Cd^{2+} concentration in the solution was determined according to the ASTM (D3557-90 method) (ASTM 2012) using atomic absorption spectrophotometry (Analytikjena, vario 6, Germany) at a wavelength of 228.8 nm. Herein, all measurements were performed in an air/acetylene flame. The lamp current and slit width were 2.0 mA and 1.2 nm, respectively. The instrument was calibrated with a standard solution (in the range 0.05–2.0 mg/L) within a linear range, and a high correlation coefficient ($R^2 > 0.997$) was obtained. All experiments were performed in duplicate and the results were reported as the mean values of measurements.

The amount of the Cd^{2+} adsorbed on CS@NZVI, q_e (i. e. adsorption capacity, mg/g), and the removal efficiency were calculated using the following equations:

$$Cd^2 \text{ adsorption capacity (mg/g)} = (C_i - C_e)\left(\frac{V}{m}\right) \quad (4)$$

$$Cd^2 \text{ removal efficiency (\%)} = \left(1 - \frac{C_e}{C_i}\right) \times 100 \quad (5)$$

where C_i and C_e are the initial and residual concentrations of Cd^{2+} (mg/L) in the solution, respectively, m is the dry mass of CS@NZVI (g) and V is the volume of the solution (L).

RESULTS AND DISCUSSION

Characterization of CS@NZVI

XRD can provide very useful information about the physical and chemical structures of the magnetic particles embedded in the CS matrix. The XRD spectra of CS@NZVI in the 2θ range of 0–80 ° at 25 °C (Cu Kα, $\lambda = 1.54$ Å) are shown in Figure 1(a). A narrow diffraction peak at $2\theta = 44.9$ ° was observed, belonging to NZVI crystal (JCPDS, No. 06-0696) (Fu *et al.* 2013; Babaei *et al.* 2015a). This confirms that the NZVI particles were successfully synthesized. In addition, the X-ray pattern of CS@NZVI exhibited characteristic crystalline peaks belonging to CS at $2\theta = 8$ ° and 20.1 ° (Jagtap *et al.* 2011; Mohseni-Bandpi *et al.* 2015). These results suggest that the NZVI particles were successfully loaded on either the outside or inside of CS.

The results of TEM analysis, Figure 1(b), showed that NZVI had a diameter less than 50 nm and also demonstrated that it was successfully synthesized as individual nano-sized particles. The specific surface area, volume, and average pore diameter of CS@NZVI were measured using the BET method. The surface of the synthesized adsorbent, according to this analysis, was 78.3 m^2/g. It is notable that the specific surface area of CS decreased after the coating of NZVI, as reported in the literature (Babaei *et al.* 2015a). This decrease may result from the impregnation process and/or NZVI presence in the structure of CS. Similar observations were also reported by other researchers (Kakavandi *et al.* 2014, 2015). The average size and volume pores of the composite were obtained to be 26.57 nm and 0.982 cc/g, respectively. According to the IUPAC classification, the average size of 26.57 nm can be classified as mesoporous groups (Depci 2012). The results of this analysis reveal that the CS@NZVI is porous in structure and could provide

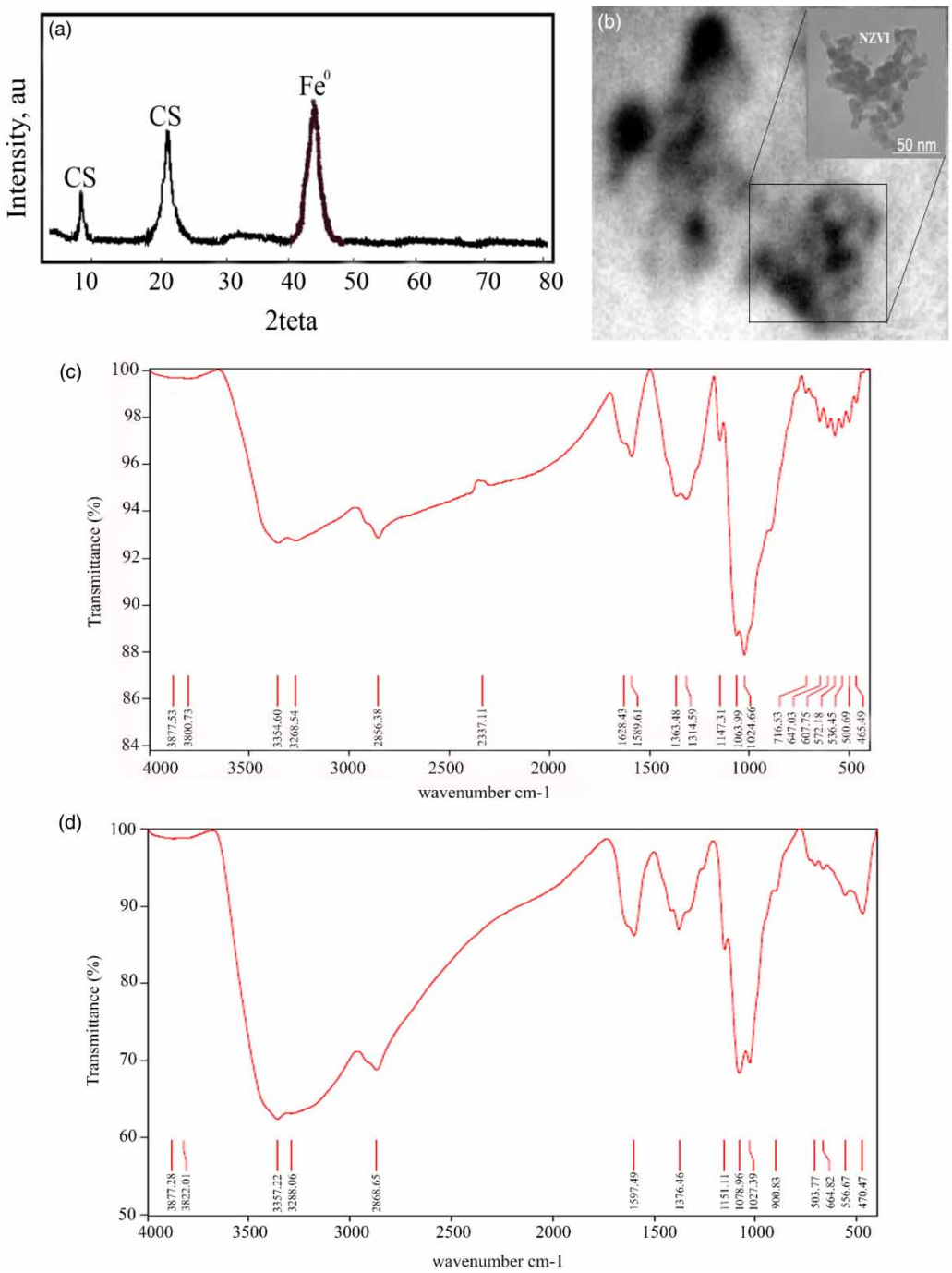

Figure 1 | (a) Powder XRD pattern, (b) TEM image of CS@NZVI, (c) FTIR spectra of CS@NZVI before, and (d) after Cd^{2+} adsorption.

more reactive sites and a good adsorption capacity for contaminants. Because adsorption reactions mainly occurred on the adsorbent surfaces, the functional groups on the surfaces of the adsorbent can play a significant role in the adsorption process. To characterize the functional groups on the surfaces of the adsorbent and to measure the binding mechanism of the pollutants, the FTIR spectra of the CS@NZVI before and after adsorption of Cd^{2+} in the

range of 400–4,000 cm^{-1} are shown in Figure 1(c) and 1(d), respectively.

The FTIR spectra showed some absorption peaks belonging to various functional groups or different vibration modes. A comparison between the FTIR spectrums of the CS@NZVI before and after the adsorption of Cd^{2+} is given in Table 1. The absorption bonds at wave number (ν) values at ~3,354 and ~3,268 cm^{-1} indicate the presence of O–H and N–H bond stretching, respectively. The absorption peaks at 2,860 cm^{-1} are due to the C–H stretching vibration of the $-CH_2$ groups in CS (Du *et al.* 2014; Mohseni-Bandpi *et al.* 2015). The peak observed at 1,631 cm^{-1} may be from the N-H bending vibration, indicating the existence of amide(II) and hydroxyl groups in CS (Liu *et al.* 2012). Moreover, the bond at near 1,600 cm^{-1} that appeared on CS@NZVI before and after adsorption of 10 mg/L Cd^{2+} was assigned to the OH bending vibrational mode due to the adsorption of moisture when FTIR sample disks were prepared in an open-air atmosphere (Mohseni-Bandpi *et al.* 2015). The bands at about 1,363 cm^{-1} can be attributed to C–N stretching vibration (Malkoc & Nuhoglu 2006). In the FTIR spectra, the peaks at around 1,140 cm^{-1} can be apportioned to the C= O stretching of ether groups (Malkoc & Nuhoglu 2006). The peaks at 1,083 cm^{-1} and 1,023 cm^{-1} correspond to C–OH bond stretching (Reddy & Lee 2013). The peaks at around 570 cm^{-1} in the CS@NZVI spectrum were attributed to the Fe–O stretching vibration, implying that the NZVI nanoparticles were successfully prepared and introduced into the CS (Yang *et al.* 2014).

In the CS@NZVI spectrum after adsorption, a significant reduction of absorption in this spectral area can be attributed to the formation of CS – Fe bonds. All the aforementioned peaks were also observed in the 'after adsorption' FTIR spectra with notable changes. These functional groups may form surface complexes with Cd^{2+} and thus can increase the specific adsorption of Cd^{2+} by CS@NZVI. As shown in Figure 1(c) and 1(d) and Table 1, the spectra display a number of absorption peaks, indicating the complex nature of the CS@NZVI. Large changes are clearly observed on the FTIR spectrum of CS@NZVI following Cd^{2+} adsorption. After Cd^{2+} adsorption, the FTIR spectrum, Figure 1(d), shows a new strong peak at 2,868 cm^{-1}, belonging to the stretching vibration of symmetric and asymmetric $-CH_2$ groups (Ngah *et al.* 2008). Furthermore, FTIR spectra of Cd^{2+} adsorbed on CS@NZVI indicated that the peaks expected at 3,354, 3,268, 2,856, 1,589, 1,363 and 1,147 cm^{-1} had shifted, respectively to 3,357, 3,288, 2,868, 1,597, 1,376 and 1,151 cm^{-1} due to Cd^{2+} sorption. It seems that the mentioned functional groups influence the Cd^{2+} adsorption on the CS@NZVI. Generally, the findings of FTIR studies clearly confirm the existence of CS and NZVI in the CS@NZVI composite.

Table 1 | The FTIR spectral characteristics of CS@NZVI before and after Cd^{2+} adsorption

	Frequencies (cm^{-1})				
IR peaks	**Before adsorption**	**After adsorption**	**Differences**	**Assignment**	**References**
1	3,354–3,268	3,357–3,288	–3, –20	O–H bond stretching and N–H bond stretching	Babaei *et al.* (2015b), Mohseni-Bandpi *et al.* (2015)
3	2,856	2,868	–12	C–H stretching vibration of the $-CH_2$ groups	Viswanathan & Meenakshi (2010), Mohseni-Bandpi *et al.* (2015)
4	1,589	1,597	–8	OH bending vibrational	Mohseni-Bandpi *et al.* (2015)
5	1,363	1,376	–4	C–N stretching vibration	Malkoc & Nuhoglu (2006)
6	1,147	1,151	+6	C = O stretching of ether groups	Malkoc & Nuhoglu (2006)
7	1,063	1,078	–3	C–OH bond stretching	Reddy & Lee (2013)
8	1,024	1,027	–3	C–OH bond stretching	Reddy & Lee (2013)
9	572	556	16	Fe–O stretching vibration	Yang *et al.* (2014)

Influence of initial solution pH

The pH of the solution, affecting the surface functional groups of the adsorbent and adsorbate, is one of the most influential parameters of the adsorption process. The dominant forms of heavy metals in aqueous solution were also affected by pH (Kakavandi *et al.* 2016b). It has been previously reported that the efficiency of heavy metals adsorption is highly dependent on the initial pH of the solution. Similar results were also observed in our work, which are illustrated in Figure 2. As can be seen, Cd^{2+} adsorption percentages enhanced with an increase in the pH from 4 to 8 for 10 mg/L Cd^{2+} concentration during 90 min agitation time. The removal efficiency then decreased significantly, when the pH value reached 9.0. Figure 2 indicates that the adsorption of Cd^{2+}on CS@NZVI is favored at around neutral pH values, which can be attributed to the changes of surface properties of the adsorbent and adsorbate. A maximum Cd^{2+} uptake was observed at a solution pH of 8.0. At acidic conditions (pH < 5), the surface of the adsorbent is positive and so, electrostatic repulsion occurs between protons (H^+) and Cd^{2+} cations for the adsorption sites. Therefore, competition between protons and metal species could be a reason for the weak adsorption in this condition. After 90 min reaction, removal efficiencies of 96.5%, 97.6% and 98% were obtained when pH values of the solution were 6.0, 7.0 and 8.0, respectively, indicating that the changes of the removal efficiency is not notable. Hence, to ensure the interference from metal precipitation we set the pH of solutions at 7.0 for the following experiments. This would allow for Cd^{2+} removal in wastewater without pre-adjustment of pH. These results are in good agreement with those of previous studies for several sorbent-Cd^{2+} sorption processes (Ünlü & Ersoz 2007; Wang *et al.* 2010; Liu *et al.* 2013). Azouaou *et al.* (2010) in studying Cd^{2+} adsorption shows that at pH 7 the numbers of competing hydrogen ions are lower and more ligands are exposed with negative charges, resulting in greater cadmium sorption.

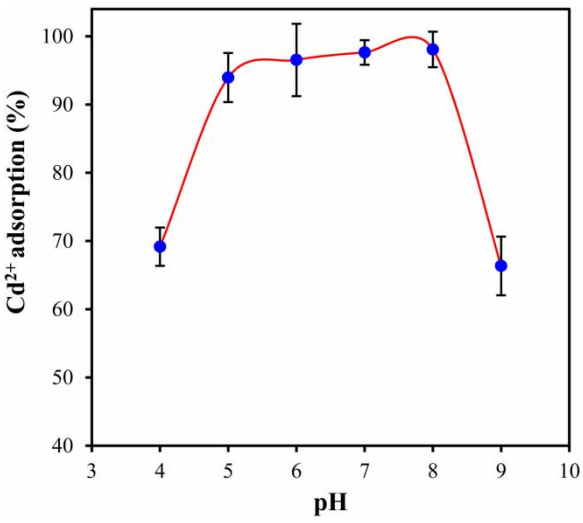

Figure 2 | Effect of solution pH on the adsorption of Cd^{2+} on CS@NZVI (Experimental conditions: adsorbent dose = 0.6 g/L; C_0 = 10 mg/L; contact time = 90 min; and T = 25 ± 1 °C).

Liu *et al.* (2013) studied the Cd^{2+} adsorption on CS beads-supported Fe^0 and showed that when solution pH increased, the number of negatively charged sites was improved, leading to the enhanced attraction force between heavy metals (Cu^{2+}, Cd^{2+} and Pb^{2+}) and the beads surface. Furthermore, Azari *et al.* (2015) reported that as the pH increased, surface positive charges of the adsorbent decreased and the more active surface sites can be obtained for Cd^{2+}, which resulted in lower repulsion of the adsorbing metal ions. At alkaline conditions, however, a decrease in the adsorption efficiency can be derived from the formation of metal hydroxides precipitation and also a decrease in the concentration of Cd^{2+}, as reported in the literature (Kakavandi *et al.* 2015). Rao *et al.* (2009) reported that at pH > 7.5, the predominant species of Cd exists in the hydrolyzed form (i.e. $Cd(OH)^+$ and $Cd(OH)_2^0$) and Cd^{2+} ions are present in only very small amounts. Therefore, at the value of pH < 7.0, the main species adsorbed onto the CS@NZVI were predominantly Cd^{2+} and less amounts of $Cd(OH)^+$ and $Cd(OH)_2$. Based on the aforementioned, at the optimum pH the predominant species of Cd were in ionic form (Cd^{2+}) and metal hydroxide precipitation does not take place.

Influence of adsorbent dosage

The dosage of CS@NZVI as a factor influencing the adsorption of Cd^{2+} was also investigated. It was examined in the range of 0.2–0.7 g/L at this condition: 10 mg/L of Cd^{2+} over 90 min at pH 7.0 ± 0.2. As shown in Figure 3(a), by raising adsorbent dosage from 0.2 to 0.7 g/L, the removal percentage of Cd^{2+} ions significantly increased from 81.7

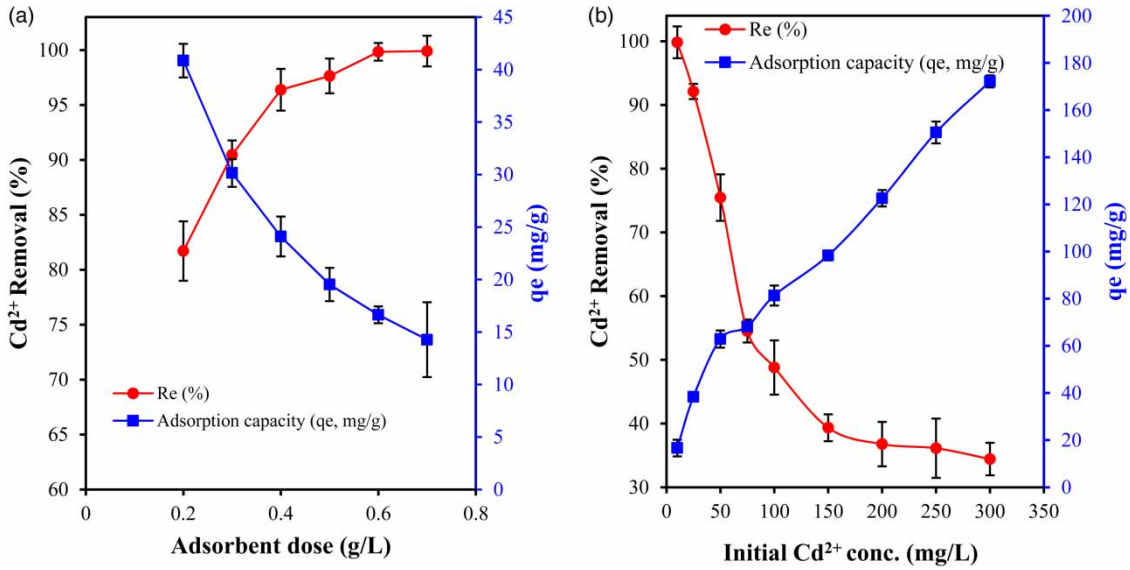

Figure 3 | Effect of (a) adsorbent dose and (b) initial Cd^{2+} concentration on adsorption capacity and removal of Cd^{2+} by CS@NZVI. Experimental conditions: pH = 7.0 ± 0.2; contact time = 90 min; and T = 25 ± 1 °C; for (a) C_0 = 10 mg/L; for (b) adsorbent dose = 0.6 g/L.

to 99.9%, while the adsorption capacity (the amount adsorbed per unit mass of adsorbent) declined from 40.8 to 14.3 mg/g. The promotion of sorption efficiency can be explained by the fact that increasing the adsorbent dosage increased the accessibility of active sites on the pores of the CS@NZVI to the Cd^{2+} ions, which led to an enhanced removal efficiency, as observed by the other researchers (Rao *et al.* 2009; Azari *et al.* 2015). In other words, for a fixed initial adsorbate concentration, increasing adsorbent dosage provides greater surface area or more adsorption sites. As shown in Figure 3(a), the complete removal of Cd^{2+} was approximately achieved at high adsorbent dosage level (0.7 g/L). The experiments also indicated that the removal efficiency was faster as the adsorbent dosage raised from 0.2 to 0.6 g/L. According to Figure 3(a), a removal efficiency of 99.8 and 99.9% was obtained in the presence of 0.6 and 0.7 g/L, respectively, of CS@NZVI in the Cd^{2+} solution, demonstrating that beyond the 0.6 g/L dosage the removal efficiency did not change with the adsorbent dose. Hence, 0.6 g/L was chosen as the optimal dosage of the adsorbent to conduct further experiments on the adsorption process.

However, a decrease in adsorption capacity with an increase in the adsorbent dosage is mainly attributed to the increase in unsaturation of adsorption sites through the adsorption reaction (Jafari *et al.* 2016; Kakavandi *et al.* 2016a). In addition, some of the particle interactions (e.g. aggregation) which result from a high sorbent concentration lead to a significant reduction in the active surface area of the adsorbent and, consequently, reduce its adsorption capacity. Similar observations have been reported for adsorption of Cd^{2+} onto the different adsorbents in the literature (Rao *et al.* 2009; Shen *et al.* 2009; Azari *et al.* 2015).

Influence of initial Cd^{2+} concentration

The effect of initial concentrations of Cd^{2+} on its removal efficiency by CS@NZVI in the range of 10-300 mg/L is shown in Figure 3(b). It can be seen that the removal efficiency decreased with enhancement of the Cd^{2+} from 10 to 300 mg/L. So that, with the rise in the initial concentration from 10 to 300 mg/L, the removal efficiency decreased from 99.8% to 34.4%. This is probably due to the fixed number of active sites on the adsorbent versus the number of metal ion molecules (Teymouri *et al.* 2013). Figure 3(b) also reveals that the adsorption capacity of Cd^{2+} on the CS@NZVI significantly enhanced as the initial Cd^{2+} concentration increased. This phenomenon can be described by the fact that amounts of Cd^{2+} adsorbed per unit mass of CS@NZVI increase with an increase in initial

Cd^{2+} concentration in the solution. Moreover, an increase in initial concentration dramatically enhanced the interaction between the adsorbent and Cd^{2+}. This can be attributed to the increased force of concentration gradient (Kumar *et al.* 2009).

Generally, at higher initial concentration of metal ions the available adsorption sites of the CS@NZVI become fewer and the percent removal of metal ions is dependent upon the initial concentration. However, the ratio of the initial number of metal ions to the available sorption sites of the CS@NZVI is decreased at a lower initial concentration of Cd^{2+}, and subsequently the fractional adsorption of metal ions by the CS@NZVI becomes independent of its initial concentration (Rao *et al.* 2009; Yang *et al.* 2014; Azari *et al.* 2015).

Influence of contact time and adsorption kinetics

The effect of contact time and adsorption kinetics were studied at a period of 3 h under optimum conditions (i.e. pH of 7.0 ± 02 and 0.6 g/L of CS@NZVI) for 10 mg/L Cd^{2+}. As shown in Figure 4(a), the adsorption capacity of Cd^{2+} increased rapidly during the first 60 min and then reached the equilibrium point after 90 min. It was observed that the rate of Cd^{2+} adsorption onto CS@NZVI was initially fast; then, the rate slowed down gradually until the equilibrium was reached, beyond which no further adsorption could be observed. Thereafter, 90 min was selected for the future experiments as the equilibrium time. The rapid increase of the adsorption capacity in the initial stages might be due to the availability of a large number of vacant sites that become saturated over time (Kakavandi *et al.* 2015). With further increasing time, the availability of the Cd^{2+} ions to unoccupied active sites on the surface of the adsorbent diminished; and these sites ultimately become saturated when the process reaches its equilibrium state. The adsorption equilibrium is the point at which the concentration of the adsorbate in the bulk solution is in a dynamic balance with that of the interface (Kakavandi *et al.* 2016b).

In Table 2, the values of the kinetic model parameters of Cd^{2+} adsorption onto CS@NZVI are listed. In this study, we used four widely used kinetic models: pseudo-first-order, pseudo-second-order, Elovich, and intraparticle diffusion models to estimate overall sorption rates. Further details of these models (i.e. equations and parameters) are given in the supplementary data, Table S1 (available with the online version of this paper). The correlation coefficients were found to be less than 0.96, 0.85 and 0.67 for the

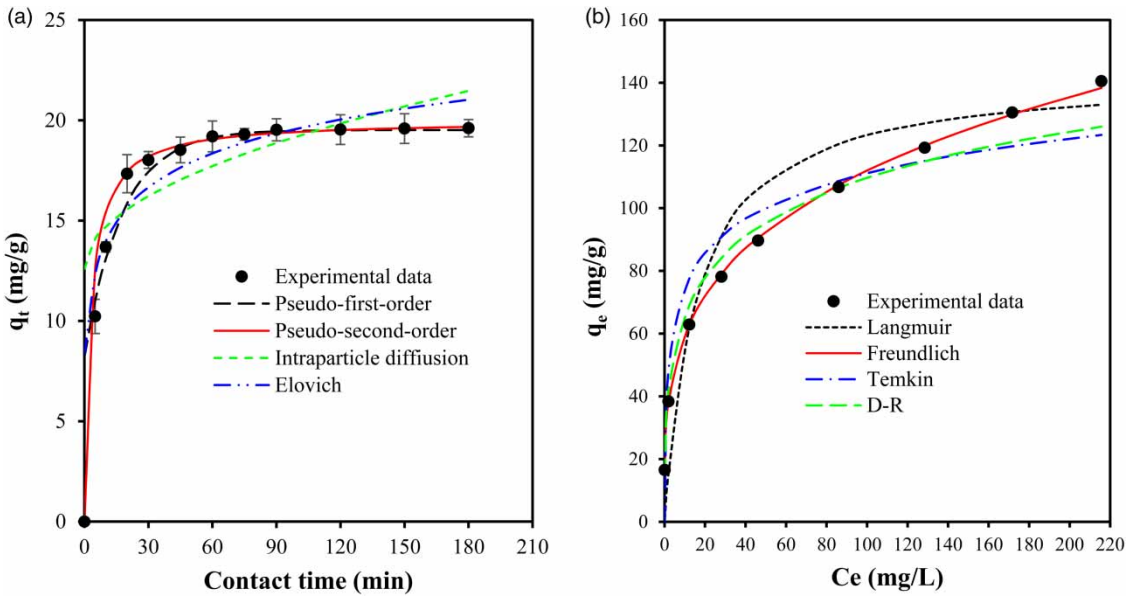

Figure 4 | (a) Kinetic and (b) isotherm models and experimental data of Cd^{2+} adsorption on CS@NZVI under optimum conditions (pH = 7.0 ± 0.2; adsorbent dose = 0.6 g/L and T = 25 ± 1 °C; for (a) C_0 = 10 mg/L; for (b) C_0 = 10-300 mg/L and contact time = 90 min).

Table 2 | The values of kinetics and isotherms of Cd^{2+} adsorption on CS@NZVI

Models	Parameters	Value
Kinetic		
Pseudo-first-order		
$ln(q_e\text{-}q_t) = lnq_e\text{-}k_1\ t$	$q_{e,cal}$ (mg/g)	11.25
	k_f (min^{-1})	0.056
	R^2	0.9519
Pseudo-second-order		
$t/q_t = t/q_e + 1/k_2\ q_e^2$	$q_{e,cal}$ (mg/g)	20
	k_s (g/mg min)	0.016
	R^2	0.9999
Intraparticle diffusion		
$q_t = k_i\ t^{0.5}$	k_i ($mg/gmin^{0.5}$)	0.6415
	C_i (mg/g)	12.61
	R^2	0.66
Elovich		
$q_t = \beta\ ln(\alpha\beta) + \beta\ lnt$	α (mg/g min)	12.73
	β (g/mg)	2.44
	R^2	0.8479
	$q_{e,exp}$ (mg/g)	19.52
Isotherm		
Freundlich		
$lnq_e = lnk_F + n^{-1}\ lnC_e$	k_F ($mg/g(Lmg)^{1/n}$)	31.5
	n	3.63
	R^2	0.9998
Langmuir		
$C_e/q_e = C_e/q_0 + 1/k_L q_0$	q_0 (mg/g)	142.8
	k_L (L/mg)	0.062
	R_L	0.05 - 0.61
	R^2	0.9816
Temkin		
$q_e = B_1\ ln\ K_T + B_1\ ln\ C_e$	q_m (mg/g)	15.96
	k_T	10.5
	R^2	0.9113
D-R		
$ln\ q_e = ln\ q_m\text{-}D\varepsilon^2$	q_m (mol/g)	215.1
	D (mol^2/kJ^2)	0.0023
	E (kJ/mol)	14.74
	R^2	0.9865

pseudo-first-order, Elovich and intraparticle diffusion kinetic models, respectively; whereas the corresponding amount calculated for the pseudo-second-order kinetic model was more than 0.999. This suggests that the pseudo-second-order is a better fit to the experimental data of Cd^{2+} adsorption with a significantly high coefficient of correlation (R^2) (>0.99), compared to other kinetic models. For the pseudo-second-order model it is also strongly confirmed that the calculated q_e values are in good agreement with the experimental q_e values, indicating that this model better explains the adsorption process of Cd^{2+} on the CS@NZVI than the other models. The confirmation of this model demonstrates that the concentrations of both adsorbent and adsorbate are associated with the rate-determining step of the adsorption process (Jafari *et al.* 2016). It also suggests that chemisorption was the rate-limiting step in the adsorption process of Cd^{2+} onto the CS@NZVI, and there was no mass transfer reaction (Kakavandi *et al.* 2014). In the previous studies conducted, the same model for the adsorption of Cd^{2+} on various adsorbents, such as magnetic activated carbon (Azari *et al.* 2015), activated carbon (Rao *et al.* 2009) (Dong *et al.* 2014), and clarified sludge (Naiya *et al.* 2008) were reported.

Other models (i.e. pseudo-first-order, Elovich and intraparticle diffusion) present lower R^2 values, indicating that these models could not properly fit the experimental kinetic data. Based on the results, it was found that the intraparticle diffusion model plays a less significant role in the adsorption process. According to Table 2, for intraparticle diffusion the y-intercept (C_i) is not zero, illustrating that the intraparticle diffusion is part of the adsorption but not the only rate-controlling step in this process, as reported previously by Boparai *et al.* (2011). Therefore, it can be stated that other mechanisms (i.e. complexes or ion-exchange) could also control the rate of the adsorption of Cd^{2+} on CS@NZVI.

Adsorption equilibrium and isotherm study

In this study, Langmuir, Freundlich, Temkin and Dubinin–Radushkevich (D-R) equilibrium as the four most common isotherm models were employed to predict the behavior of Cd^{2+} adsorption onto the CS@NZVI surfaces. The equations and corresponding parameters of the aforementioned models are represented in Table S1. The adsorption isotherm experiments were conducted using 10 to 300 mg/L Cd^{2+} under the optimum conditions (i.e. pH 7.0 ± 0.2, 0.6 g/L adsorbent and 90 min contact time) at 25 ± 1 °C. Table 1 shows the

obtained values of equilibrium isotherm parameters of the Cd^{2+} adsorption onto the CS@NZVI surfaces. Based on the correlation coefficients (R^2), the adsorption isotherm models fitted the experimental data in accordance to the following order: Freundlich > D-R > Langmuir > Temkin. Considering this result, the Freundlich model is a better fit to the experimental data of the Cd^{2+} adsorption by CS@NZVI than the other three models. In addition, we observed the best fit for the Freundlich model by employing a nonlinear method, as plotted in Figure 4(b). This model suggests that the heterogeneous functional sites are distributed uniformly on the surfaces of CS@NZVI and the adsorption of Cd^{2+} ions onto non-energetically equivalent sites of the CS@NZVI (Kakavandi *et al.* 2015; Rezaei Kalantry *et al.* 2016). Meanwhile, the value of 1/n (less than unity) in the Freundlich isotherm model implies the favorable adsorption of Cd^{2+} onto CS@NZVI. In addition, as presented in Table 2, the values for the dimensionless separation parameter R_L ($R_L = 1/(1 + k_L C_0)$), which were related to the Langmuir model, fell between 0 and 1. Since $R_L > 1$, $R_L = 1$, $R_L = 0$ and $0 < R_L < 1$ indicate unfavorable, linear, irreversible and favorable adsorption, respectively, it can be concluded that the simultaneous adsorption of Cd^{2+} onto CS@NZVI is favorable.

For the D-R model, the mean free energy of adsorption ($E = 1/(-2D)^{0.5}$) per mole of the adsorbate is the energy needed to transfer one mole of an adsorbate to the adsorbent surfaces from infinity in solution. It gives information about either chemical or physical adsorption. With the magnitude of E, between 8 and 16 kJ/mol, the adsorption mechanism follows chemical ion-exchange, while for the values of E < 8 kJ/mol, the adsorption process is of a physical nature (Azouaou *et al.* 2010; Kakavandi *et al.* 2015). As shown in Table 2, the value of the mean free energy of adsorption, E, for Cd^{2+} on CS@NZVI, was found to be between 8 and 16 kJ/mol, indicating that the adsorption process follows a chemical mechanism. The chemisorption nature of Cd^{2+} adsorption on different types of adsorbents has been reported previously (Ünlü & Ersoz 2007; Naiya *et al.* 2008; Boparai *et al.* 2011).

The maximum adsorption capacity, q_m, of the CS@NZVI was compared with the other adsorbents (see Table 3). It is worth mentioning that the CS@NZVI poses a better adsorption capacity, compared with the capacity of other adsorbents applied in previous research. The observed differences in the adsorption capacities for the listed adsorbents can be due to the structure, surface area and the properties of the functional groups in each adsorbent. As presented in Table 3, α-ketoglutaric acid-modified magnetic CS provides a high adsorption capacity for Cd^{2+} compared with other adsorbents, which can be attributed to its textural characteristics, high porosity and surface area and functional groups. Moreover, it is worth noting from this table that the CS@NZVI had a positive effect on Cd^{2+} removal and can be considered as one of the most effective adsorbents for Cd^{2+} adsorption. Nevertheless, in order to enhance the adsorption capacity of CS@NZVI, further studies can be conducted on its modification through increasing the surface area and changing of functional groups.

Regeneration and reusability of CS@NZVI

The regeneration of the adsorbent and the restoration of adsorption are crucial factors in the applicability of a typical adsorbent. In this study, regeneration and the reusability experiments of Cd^{2+} on the CS@NZVI were assessed under the optimum conditions through three successive cycles. To regenerate the spent CS@NZVI at the end of each adsorption cycle for the next adsorption, the used adsorbent was collected magnetically and stirred in DI-water for 90 min. The adsorbent was subsequently filtered and dried overnight for the next use. For desorption experiments, 0.10 g of CS@NZVI loaded with Cd^{2+} was then shaken at 200 rpm for 90 min with 5 mL of DI-water at 25 ± 1 °C. The regenerated adsorbent was then dried in an oven at 100 °C for 2 h and used for the next adsorption–desorption cycle, in order to test the reusability of CS@NZVI for Cd^{2+} removal. At the end of each adsorption/desorption cycle, the desorption percentage (%) was calculated using Equation (6).

$$\text{Desorption (\%)} = \left(\frac{\text{Amount of } Cd^{2+} \text{ desorbed}}{\text{Amount of } Cd^{2+} \text{ adsorbed}}\right) \times 100 \qquad (6)$$

As can be seen from Figure 5, the adsorption percentages of Cd^{2+} by CS@NZVI slightly dropped from 99.8%

Table 3 | Maximum adsorption capacity and optimum conditions of different adsorbents for Cd^{2+} removal

Adsorbent	pH	Isotherm	Kinetic	q_m (mg/g)	References
Ion-imprinted carboxymethyl CS-functionalized silica gel	5.0	-	Pseudo-second-order	20.7	Lü *et al.* (2013)
Crosslinked CS/poly(vinyl alcohol) beads	6.0	Langmuir and Freundlich	Pseudo-second-order	142.9	Kumar *et al.* (2009)
α-Ketoglutaric acid-modified magnetic CS	6.0	Langmuir	Pseudo-first-order	255.7	Yang *et al.* (2014)
Activated carbon prepared from *Phaseolus aureus* hulls	8.0	Freundlich	Pseudo-second-order	15.7	Rao *et al.* (2009)
Magnetic activated carbon	5.7	Langmuir	Pseudo-second-order	63.52	Azari *et al.* (2015)
Clarified sludge	5.0	Langmuir	Pseudo-second-order	36.23	Naiya *et al.* (2008)
Dithiocarbamated-sporopollenin	7.0	Langmuir	Pseudo-second-order	7.1	Ünlü & Ersoz (2007)
Untreated coffee grounds	7.0	Freundlich	Pseudo-second-order	15.65	Azouaou *et al.* (2010)
Untreated *Pinus halepensis* sawdust	9.0	Freundlich	Pseudo-second-order	5.36	Semerjian (2010)
Oxidized granular activated carbon	6.0	Langmuir	Pseudo-second-order	5.73	Huang *et al.* (2007)
NaCl-treated *Ceratophyllum demersum*	6.0	Langmuir	Pseudo-second-order	35.7	Jaafarzadeh *et al.* (2014)
CS@NZVI	7.0	Freundlich	Pseudo-second-order	142.8	This study

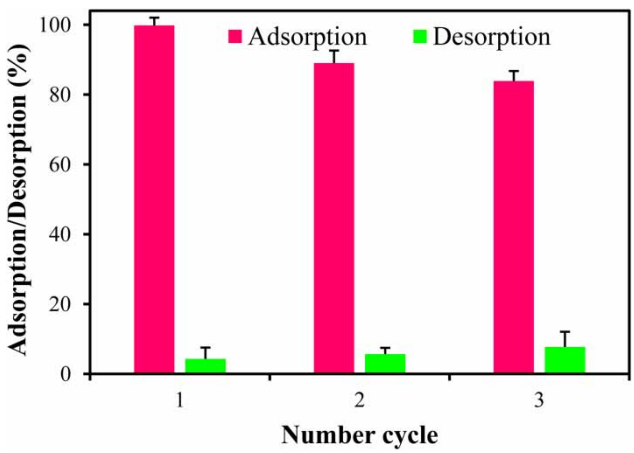

Figure 5 | Reusability and regeneration results for the adsorption of Cd^{2+} by CS@NZVI composite in aqueous solution.

to 83.9%. This suggests that the CS@NZVI can be reused for at least three successive cycles while maintaining high adsorption efficiency. As implied in Figure 5, however, the desorption percentage of DI-water is very low for all studied cycles. This means that DI-water is not suitable to be used as a desorbent solution for the regeneration of CS@NZVI loaded with Cd^{2+} ions. It seems that some desorbent solutions such as HCl, NaCl, NaOH and methanol could provide a good potential for regeneration of CS@NZVI.

CONCLUSIONS

Results revealed that CS@NZVI has a high potential and adsorption capacity for Cd^{2+} ion removal from aqueous solutions. At a pH of 7 ± 0.2, the adsorption efficiency was enhanced by an increase in the contact time and adsorbent dosage and a decrease in the initial Cd^{2+} concentration. The equilibrium adsorption data were found to fit best using a Freundlich isotherm and pseudo-second-order kinetic models. The maximum adsorption capacity obtained was 142.8 mg/g based on the Langmuir isotherm. The adsorption process of Cd^{2+} onto the synthesized composite was chemisorption. Moreover, the adsorbent was successfully recycled for three cycles with a little decrease of variation in adsorption ability. The CS@NZVI provides very promising results for cost-effective treatment of wastewaters contaminated by Cd^{2+}, as well as high adsorption capacities,

good and rapid separations and an efficient technology for heavy metals removal.

ACKNOWLEDGEMENTS

The present work was financially supported by the Environmental Technologies Research Center, Ahvaz Jundishapur University of Medical Sciences (Grant No. ETRC-9112). The authors are grateful for the support of Iranian Nano Technology Initiative Council.

REFERENCES

Ahmadi, M., Teymouri, P., Setodeh, A., Mortazavi, M. S. & Asgari, A. 2011 Adsorption of Pb(II) from aqueous solution onto Lewatit FO36 nano resin: equilibrium and kinetic studies. *Environmental Engineering & Management Journal (EEMJ)* **10**, 1579–1587.

Al Sagheer, F., Al-Sughayer, M., Muslim, S. & Elsabee, M. Z. 2009 Extraction and characterization of chitin and chitosan from marine sources in Arabian Gulf. *Carbohydrate Polymers* **77**, 410–419.

American Society for Testing and Material (ASTM) 2012 *Standard Test Methods for Cadmium in Water, Methods D3557-12 and D3557-90*. ASTM, Pennsylvania, USA.

Amiri, H., Jaafarzadeh, N., Ahmadi, M. & Martínez, S. S. 2011 Application of LECA modified with Fenton in arsenite and arsenate removal as an adsorbent. *Desalination* **272**, 212–217.

Azari, A., Kakavandi, B., Kalantary, R. R., Ahmadi, E., Gholami, M., Torkshavand, Z. & Azizi, M. 2015 Rapid and efficient magnetically removal of heavy metals by magnetite-activated carbon composite: a statistical design approach. *Journal of Porous Materials* **22**, 1083–1096.

Azouaou, N., Sadaoui, Z., Djaafri, A. & Mokaddem, H. 2010 Adsorption of cadmium from aqueous solution onto untreated coffee grounds: equilibrium, kinetics and thermodynamics. *Journal of Hazardous Materials* **184**, 126–134.

Babaei, A. A., Azari, A., Kalantary, R. R. & Kakavandi, B. 2015a Enhanced removal of nitrate from water using nZVI@ MWCNTs composite: synthesis, kinetics and mechanism of reduction. *Water Science and Technology* **72** (11), 1988–1999.

Babaei, A. A., Khataee, A., Ahmadpour, E., Sheydaei, M., Kakavandi, B. & Alaee, Z. 2015b Optimization of cationic dye adsorption on activated spent tea: equilibrium, kinetics, thermodynamic and artificial neural network modeling. *Korean Journal of Chemical Engineering* **33**, 1352–1361.

Begum, S. A., Golam Hyder, A. H. M. & Vahdat, N. 2016 Adsorption isotherm and kinetic studies of As(V) removal from aqueous solution using cattle bone char. *Journal of Water Supply: Research and Technology – Aqua* **65**, 244–252.

Boparai, H. K., Joseph, M. & O'Carroll, D. M. 2011 Kinetics and thermodynamics of cadmium ion removal by adsorption onto nano zerovalent iron particles. *Journal of Hazardous Materials* **186**, 458–465.

Brown, D. 2015 *Method for Chitosan Production*. US Patent 20,150,167,03, USPTO, Alexandria, VA.

Chen, C., Hu, J., Shao, D., Li, J. & Wang, X. 2009 Adsorption behavior of multiwall carbon nanotube/iron oxide magnetic composites for Ni(II) and Sr(II). *Journal of Hazardous Materials* **164**, 923–928.

Depci, T. 2012 Comparison of activated carbon and iron impregnated activated carbon derived from Gölbaşı lignite to remove cyanide from water. *Chemical Engineering Journal* **181**, 467–478.

Dong, C., Chen, W. & Liu, C. 2014 Preparation of novel magnetic chitosan nanoparticle and its application for removal of humic acid from aqueous solution. *Applied Surface Science* **292**, 1067–1076.

Du, Y., Pei, M., He, Y., Yu, F., Guo, W. & Wang, L. 2014 Preparation, characterization and application of magnetic Fe_3O_4-CS for the adsorption of orange I from aqueous solutions. *PLoS One* **9** (10), e108647.

Esfahani, A. R., Firouzi, A. F., Sayyad, G. & Kiasat, A. 2014a Transport and retention of polymer-stabilized zero-valent iron nanoparticles in saturated porous media: effects of initial particle concentration and ionic strength. *Journal of Industrial and Engineering Chemistry* **20**, 2671–2679.

Esfahani, A. R., Hojati, S., Azimi, A., Farzadian, M. & Khataee, A. 2014b Enhanced hexavalent chromium removal from aqueous solution using a sepiolite-stabilized zero-valent iron nanocomposite: impact of operational parameters and artificial neural network modeling. *Journal of the Taiwan Institute of Chemical Engineers* **49**, 172–182.

Fan, L., Luo, C., Lu, Z., Lu, F. & Qiu, H. 2011 Preparation of magnetic modified chitosan and adsorption of Zn^{2+} from aqueous solutions. *Colloids and Surfaces B: Biointerfaces* **88**, 574–581.

Fan, L., Luo, C., Sun, M., Li, X. & Qiu, H. 2013 Highly selective adsorption of lead ions by water-dispersible magnetic chitosan/graphene oxide composites. *Colloids and Surfaces B: Biointerfaces* **103**, 523–529.

Fu, F., Ma, J., Xie, L., Tang, B., Han, W. & Lin, S. 2013 Chromium removal using resin supported nanoscale zero-valent iron. *Journal of Environmental Management* **128**, 822–827.

Geng, B., Jin, Z., Li, T. & Qi, X. 2009 Preparation of chitosan-stabilized Fe0 nanoparticles for removal of hexavalent chromium in water. *Science of the Total Environment* **407** (18), 4994–5000.

Gupta, A., Yunus, M. & Sankararamakrishnan, N. 2011a Zerovalent iron encapsulated chitosan nanospheres – a novel adsorbent for the removal of total inorganic arsenic from aqueous systems. *Chemosphere* **86**, 150–155.

Gupta, V., Agarwal, S. & Saleh, T. A. 2011b Chromium removal by combining the magnetic properties of iron oxide with

adsorption properties of carbon nanotubes. *Water Research* **45**, 2207–2212.

Hu, J., Shao, D., Chen, C., Sheng, G., Li, J., Wang, X. & Nagatsu, M. 2010 Plasma-induced grafting of cyclodextrin onto multiwall carbon nanotube/iron oxides for adsorbent application. *The Journal of Physical Chemistry B* **114** (20), 6779–6785.

Huang, X., Gao, N.-y. & Zhang, Q.-l. 2007 Thermodynamics and kinetics of cadmium adsorption onto oxidized granular activated carbon. *Journal of Environmental Sciences* **19**, 1287–1292.

Jaafarzadeh, N., Amiri, H. & Ahmadi, M. 2012 Factorial experimental design application in modification of volcanic ash as a natural adsorbent with Fenton process for arsenic removal. *Environmental Technology* **33**, 159–165.

Jaafarzadeh, N., Teymouri, P., Babaei, A. A., Alavi, N. & Ahmadi, M. 2014 Biosorption of cadmium (II) from aqueous solution by NaCl-treated Ceratophyllum demersum. *Environmental Engineering & Management Journal (EEMJ)* **13**, 763–773.

Jafari, A. J., Kakavandi, B., Kalantary, R. R., Gharibi, H., Asadi, A., Azari, A., Babaei, A. A. & Takdastan, A. 2016 Application of mesoporous magnetic carbon composite for reactive dyes removal: process optimization using response surface methodology. *Korean Journal of Chemical Engineering* **33** (10), 2878–2890.

Jagtap, S., Yenkie, M., Labhsetwar, N. & Rayalu, S. 2011 Defluoridation of drinking water using chitosan based mesoporous alumina. *Microporous and Mesoporous Materials* **142** (2), 454–463.

Kakavandi, B., Rezaei Kalantary, R., Farzadkia, M., Mahvi, A. H., Esrafili, A., Azari, A., Yari, A. R. & Javid, A. B. 2014 Enhanced chromium (VI) removal using activated carbon modified by zero valent iron and silver bimetallic nanoparticles. *Journal of Environmental Health Science and Engineering* **12**, 1–10.

Kakavandi, B., Kalantary, R. R., Jafari, A. J., Nasseri, S., Ameri, A., Esrafili, A. & Azari, A. 2015 Pb(II) adsorption onto a magnetic composite of activated carbon and superparamagnetic Fe_3O_4 nanoparticles: experimental and modeling study. *CLEAN – Soil, Air, Water* **43**, 1157–1166.

Kakavandi, B., Jahangiri-rad, M., Rafiee, M., Esfahani, A. R. & Babaei, A. A. 2016a Development of response surface methodology for optimization of phenol and p-chlorophenol adsorption on magnetic recoverable carbon. *Microporous and Mesoporous Materials* **231**, 192–206.

Kakavandi, B., Jonidi Jafari, A., Rezaei Kalantary, R., Nasseri, S., Esrafili, A., Gholizadeh, A. & Azari, A. 2016b Simultaneous adsorption of lead and aniline onto magnetically recoverable carbon: optimization, modeling and mechanism. *Journal of Chemical Technology & Biotechnology* **91**, 3000–3010.

Kumar, M., Tripathi, B. P. & Shahi, V. K. 2009 Crosslinked chitosan/polyvinyl alcohol blend beads for removal and recovery of Cd(II) from wastewater. *Journal of Hazardous Materials* **172**, 1041–1048.

Lim, A. P. & Aris, A. Z. 2014 A review on economically adsorbents on heavy metals removal in water and wastewater. *Reviews in Environmental Science and Bio/Technology* **13**, 163–181.

Liu, T., Wang, Z.-L., Zhao, L. & Yang, X. 2012 Enhanced chitosan/Fe0-nanoparticles beads for hexavalent chromium removal from wastewater. *Chemical Engineering Journal* **189–190**, 196–202.

Liu, T., Yang, X., Wang, Z.-L. & Yan, X. 2013 Enhanced chitosan beads-supported Fe(0)-nanoparticles for removal of heavy metals from electroplating wastewater in permeable reactive barriers. *Water Research* **47**, 6691–6700.

Lü, H., An, H. & Xie, Z. 2013 Ion-imprinted carboxymethyl chitosan–silica hybrid sorbent for extraction of cadmium from water samples. *International Journal of Biological Macromolecules* **56**, 89–93.

Malkoc, E. & Nuhoglu, Y. 2006 Fixed bed studies for the sorption of chromium(VI) onto tea factory waste. *Chemical Engineering Science* **61**, 4363–4372.

Mohseni-Bandpi, A., Kakavandi, B., Kalantary, R. R., Azari, A. & Keramati, A. 2015 Development of a novel magnetite-chitosan composite for the removal of fluoride from drinking water: adsorption modeling and optimization. *RSC Advances* **5**, 73279–73289.

Naghizadeh, A. 2015 Comparison between activated carbon and multiwall carbon nanotubes in the removal of cadmium (II) and chromium (VI) from water solutions. *Journal of Water Supply: Research and Technology – Aqua* **64**, 64–73.

Naiya, T., Bhattacharya, A. & Das, S. 2008 Removal of Cd(II) from aqueous solutions using clarified sludge. *Journal of Colloid and Interface Science* **325**, 48–56.

Ngah, W. W., Hanafiah, M. & Yong, S. 2008 Adsorption of humic acid from aqueous solutions on crosslinked chitosan–epichlorohydrin beads: kinetics and isotherm studies. *Colloids and Surfaces B: Biointerfaces* **65**, 18–24.

Oliveira, L. C., Rios, R. V., Fabris, J. D., Garg, V., Sapag, K. & Lago, R. M. 2002 Activated carbon/iron oxide magnetic composites for the adsorption of contaminants in water. *Carbon* **40**, 2177–2183.

Oliveira, L. C., Petkowicz, D. I., Smaniotto, A. & Pergher, S. B. 2004 Magnetic zeolites: a new adsorbent for removal of metallic contaminants from water. *Water Research* **38**, 3699–3704.

Rao, M. M., Ramana, D., Seshaiah, K., Wang, M. & Chien, S. 2009 Removal of some metal ions by activated carbon prepared from *Phaseolus aureus* hulls. *Journal of Hazardous Materials* **166**, 1006–1013.

Reddy, D. H. K. & Lee, S.-M. 2013 Application of magnetic chitosan composites for the removal of toxic metal and dyes from aqueous solutions. *Advances in Colloid and Interface Science* **201**, 68–93.

Rezaei Kalantry, R., Jonidi Jafari, A., Esrafili, A., Kakavandi, B., Gholizadeh, A. & Azari, A. 2016 Optimization and evaluation of reactive dye adsorption on magnetic composite of activated carbon and iron oxide. *Desalination and Water Treatment* **57**, 6411–6422.

Semerjian, L. 2010 Equilibrium and kinetics of cadmium adsorption from aqueous solutions using untreated Pinus halepensis sawdust. *Journal of Hazardous Materials* **173**, 236–242.

Shen, Y., Tang, J., Nie, Z., Wang, Y., Ren, Y. & Zuo, L. 2009 Preparation and application of magnetic Fe_3O_4 nanoparticles

for wastewater purification. *Separation and Purification Technology* **68**, 312–319.

Sobhanardakani, S., Zandipak, R., Fili, Z., Ghoochian, M., Sahraei, R. & Farmany, A. 2015 Removal of V(V) ions from aqueous solutions using oxidized multi-walled carbon nanotubes. *Journal of Water Supply: Research and Technology – Aqua* **64**, 425–433.

Teymouri, P., Ahmadi, M., Babaei, A. A., Ahmadi, K. & Jaafarzadeh, N. 2013 Biosorption studies on NaCl-modified ceratophyllum demersum: removal of toxic chromium from aqueous solution. *Chemical Engineering Communications* **200**, 1394–1413.

Ünlü, N. & Ersoz, M. 2007 Removal of heavy metal ions by using dithiocarbamated-sporopollenin. *Separation and Purification Technology* **52**, 461–469.

Viswanathan, N. & Meenakshi, S. 2010 Enriched fluoride sorption using alumina/chitosan composite. *Journal of Hazardous Materials* **178**, 226–232.

Wang, J., Zheng, S., Shao, Y., Liu, J., Xu, Z. & Zhu, D. 2010 Amino-functionalized Fe_3O_4@SiO_2 core–shell magnetic nanomaterial as a novel adsorbent for aqueous heavy metals removal. *Journal of Colloid and Interface Science* **349**, 293–299.

World Health Organisation 2007 *Desalination for Safe Water Supply: Guidance for the Health and Environmental Aspects Applicable to Desalination.* Public Health and the Environment, World Health Organization, Geneva.

Westergren, R. 2006 *Arsenic Removal Using Biosorption with Chitosan: Evaluating the Extraction and Adsorption Performance of Chitosan from Shrimp Shell Waste*. MSC Thesis, Rotal Institute of Technology (KTH), Sweden.

Yang, G., Tang, L., Lei, X., Zeng, G., Cai, Y., Wei, X., Zhou, Y., Li, S., Fang, Y. & Zhang, Y. 2014 Cd(II) removal from aqueous solution by adsorption on α-ketoglutaric acid-modified magnetic chitosan. *Applied Surface Science* **292**, 710–716.

First received 29 April 2016; accepted in revised form 26 October 2016. Available online 30 January 2017